



Rh Nanoparticles-Decorated Graphene Oxide: An Efficient Catalyst for the Hydrogenation of Nitroaromatic Pollutants

Bagher Eftekhari-Sis¹ · Neda Pishghadam¹ · Adem Rüzgar² · Mehmet Gülcan²

Received: 20 April 2024 / Accepted: 23 May 2024

© The Author(s), under exclusive licence to Springer Science+Business Media, LLC, part of Springer Nature 2024

Abstract

Amine-functionalized graphene oxide (GO-NH₂) was prepared by synthesizing graphene oxide (GO) using the Hummer's method, followed by reacting with (3-aminopropyl)triethoxysilane (APTES). The obtained GO-NH₂ was utilized for immobilizing and stabilizing Rh(0) nanoparticles (NPs) to create Rh@GO-NH₂ material. The synthesized Rh@GO-NH₂ material was characterized using X-ray diffraction (XRD), scanning electron microscopy (SEM), energy-dispersive X-ray spectroscopy (EDS), elemental mapping, and X-ray photoelectron spectroscopy (XPS) analysis. The results indicated that the Rh(0) NPs were successfully decorated on the GO-NH₂ surface. The catalytic activity of Rh@GO-NH₂ was examined for the hydrogenation of nitroaromatic compounds using NaBH₄ as a reducing agent. Results demonstrated that Rh@GO-NH₂ effectively catalyzed the hydrogenation of nitroaromatics into the corresponding aniline derivatives in aqueous media at a moderate temperature. Nitroaromatic compounds are considered high toxic water contaminants. The simple preparation of the catalyst, low catalyst loading, and the recoverability of the catalyst are some advantages of this work.

Keywords Rh(0) NPs · Graphene oxide · Nitroarenes · Hydrogenation · Water remediation

1 Introduction

Nowadays, water is contaminated with a wide variety of chemical pollutants [1], which have adversely affected marine life and the Earth's ecosystem. Nitroaromatic organic compounds, highly toxic substances and released into the environment by the agricultural, pharmaceutical, and chemical industries, are among the most significant water-contaminating substances [2]. Therefore, it is crucial to remove these contaminants from industrial wastewater before releasing it into the environment [3, 4]. Various techniques, including adsorption, biochemical, and photocatalytic degradation methods [5–8], have been used to eliminate nitroaromatic pollutants from water and industrial wastewater. However, these methods have limitations such as the need for large

quantities of adsorbents, a time-consuming and expensive recycling and reusing process, and the potential production of other toxic substances during the degradation process [9].

Therefore, it is crucial to develop methodologies that can effectively remove nitroaromatic pollutants while also converting them into useful substances. One of the most significant methods is the hydrogenation of nitroaromatic compounds in aqueous media, which is particularly important from an environmental perspective [10]. Generally, the hydrogenation products of nitroaromatics, known as amines, are versatile and valuable intermediates in the synthesis of various biologically active natural and non-natural products. These products include drugs, polymers, sensors, corrosion inhibitors, and cosmetics, and may be of interest in synthetic and medicinal chemistry [11]. Various nitroaromatic reduction processes have been explored in the literature, including catalytic hydrogenation using H₂ or hydride donors such as LiAlH₄ and NaBH₄ in the presence of metal catalysts [12]. In recent years, supported metal NPs [13] have been widely used for the reduction of nitroaromatics, particularly 4-nitrophenol, which is considered one of the most hazardous pollutants due to its high solubility and stability in water. The reduction of nitroaromatics to their corresponding aniline derivatives by metal NPs including Ag [14–17], Rh [18], Au

✉ Bagher Eftekhari-Sis
eftekharis@maragheh.ac.ir

✉ Mehmet Gülcan
mehmetgulcan@yyu.edu.tr

¹ Department of Chemistry, University of Maragheh, Maragheh 55181-83111, Iran

² Department of Chemistry, Van Yuzuncu Yil University, Van 65080, Turkey

[19–21], Pd [22–24], Co [15], Cu [25], Ni [26], Zn [27], Fe [28], Pt [29], etc. has significantly increased.

In this context, Rahimkhoei et al. [30] developed a method for preparing and stabilizing Ag NPs on polyhedral oligomeric silsesquioxanes (POSS) cross-linked poly(*N*-isopropylacrylamide-co-itaconic acid (PNIPAM-co-IA) for converting of 4-nitrophenol into 4-aminophenol using NaBH_4 . They achieved full conversion within 10 min using 15 mg of catalyst at 50 °C. Additionally, Akbari et al. [15] described an efficient reduction of 4-nitrophenol using Ag nanoparticles on POSS-ionic liquid hybrid materials. Yavari and colleagues [14] developed Co nanoparticles supported on halloysite nanotubes modified with an ionic liquid for reducing nitroaromatics with NaBH_4 . In 2017, Bhosale et al. [31] reported that Au NPs catalyze the reduction of nitroaromatic derivatives. Nevertheless, the development of novel methodologies and catalysis for the chemoselective reduction of nitroaromatics in the presence of additional functional groups holds significant importance.

In recent years, there has been a significant increase in studies on nanocatalysts due to their exceptional effectiveness and selectivity in catalysis. Nanomaterials possess unique properties and enhanced performance based on their size, shape, and the support materials they are combined with. By using metal NPs in combination with carefully selected supports, researchers have been able to develop novel and highly active catalysts with practical industrial applications. A variety of solid supports have been used for the immobilization of metal NPs, including carbon and halloysite nanotubes, polymers [32], chitosan, cellulose, mesoporous silica [33], magnetic materials [34], and nanofibers [35]. However, the introduction of mass transfer control has only partially improved catalytic activity. Therefore, there is a continued need for the development of more efficient catalysts with suitable solid supports. Among the various solid support materials that have been investigated, graphene oxide (GO) and its various derivatives modified with functional groups have garnered significant attention due to their distinct physical and chemical characteristics and substantial surface area [36]. It is acknowledged that GO contains numerous functional groups with oxygen, such as hydroxyl, epoxy, and carboxyl groups [37]. Special attention has been placed on materials that have been functionalized with amines, as solid supports containing amine groups are known to effectively stabilize metal nanoparticles by preventing their aggregation without affecting their intrinsic characteristics, while also enhancing their catalytic efficiency [38, 39].

Rhodium NPs are utilized in a wide range of catalytic reactions due to their high stability under harsh acidic/basic and heating conditions, as well as extraordinarily high surface free energy and catalytic activity [40]. Some of the reactions catalyzed by Rh NPs include oxidation of CO,

reduction of NO and nitrate, storage of O_2 for CO_2 reforming or methane production, generation of H_2 , hydrogenation of arenes, *N*-heteroaromatics, phenols and alkenes, hydroformylation of alkenes, and electro-oxidation of alcohols. Furthermore, Rh NPs are employed in the reduction of nitroaromatic compounds [41]. In a specific study, Luo et al. [42] reported that Rh nanoparticles supported by porous ionic copolymer catalyzed the reduction of nitro compounds by hydrazine, while other functional groups such as F, Cl, Br, I, CN, NH_2 , OH, alkene, ester, and amide groups remained unchanged. Recently, a bimetallic Pt–Rh alloyed nanomultipods were constructed in oleylamine by utilizing creatinine and cetyltrimethylammonium chloride (CTAC) as co-structure-directing agents. These were then used in the catalytic reduction of 4-nitrophenol (4-NP) with NaBH_4 as the reducing reagent, achieving reduction in less than 20 min. A major drawback of this method in the preparation of the platinum–rhodium alloy using expensive precursors such as $\text{Pt}(\text{acac})_2$, $\text{Rh}(\text{acac})_3$, and creatinine at higher temperatures [43]. In a different study, Liang et al. [44] described the synthesis of Rh NPs supported on magnetically graphite-like carbon nitride ($\text{g-C}_3\text{N}_4$) and their catalytic activity in the reduction of nitroaromatic compounds using hydrazine as the reducing agent. Although the work presented the high catalytic activity of the reported Rh NPs-based catalyst in the reduction of various substituted nitroarenes, some limitations of the method include the use of a high loading (13 mg) of catalyst and a higher temperature of the reduction reaction (110 °C). Additionally, a bimetallic RhAg NPs supported on r-GO was developed for the reduction of 4-NP by NaBH_4 . The protocol used tris(triazolyl)-polyethylene glycol ligand as the stabilizing agent for AgRh NPs [45]. Also, in some cases, azoxybenzene derivatives were obtained as the main products of the nitroaromatic reduction through reductive coupling reactions [46].

Here, we conducted the synthesis and characterization of Rh(0) NPs decorated on amine-functionalized GO, referred to as Rh@GO- NH_2 , and their catalytic activity towards the hydrogenation of nitroarenes by NaBH_4 in aqueous media. The modification of GO using commercially available (3-aminopropyl)triethoxysilane (APTES), and the formation of Rh NPs from RhCl_3 precursor, along with low catalyst loading for the catalytic hydrogenation of nitroarenes, and recoverability of the catalyst are some advantages of this work.

Figure 1 illustrates a schematic representation of the preparation and catalytic activity of Rh@GO- NH_2 towards the reduction of 4-nitrophenol (4-NP). The adsorption of nitroarenes onto the GO- NH_2 , followed by the hydrogenation of the nitro group with H_2 , which is in-situ generated by Rh NPs-catalyzed decomposition of NaBH_4 , yielded corresponding aniline derivatives that desorbed from the GO- NH_2 surface.

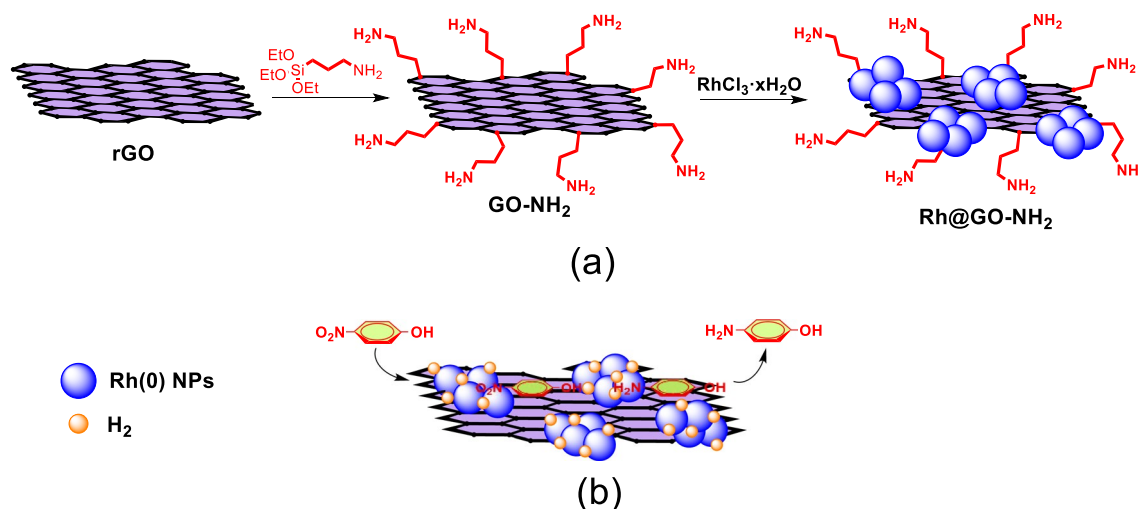


Fig. 1 Schematic representation of the preparation of Rh@GO-NH₂ (A), and Rh@GO-NH₂ catalyzed reduction of nitrophenol by NaBH₄

2 Experimental

2.1 Materials and Methods

Rhodium(III) chloride hydrate (RhCl₃·H₂O), 3-aminopropyltriethoxysilane (APTES), nitroarenes, sodium borohydride (NaBH₄), potassium permanganate (KMnO₄), sodium nitrate (NaNO₃), graphite powder, ethanol (EtOH), and toluene were obtained from Sigma-Aldrich®. All reactions and washing steps are performed with deionized water.

Inductively coupled plasma optical emission spectroscopy (ICP-OES) analysis was performed on a Perkin Elmer Optima 4300DV to determine the experimental amount of Rh in the catalyst. X-ray photoelectron spectroscopy XPS analysis was performed on a Kratos AXIS Ultra spectrometer with Al K α radiation (1486.6 eV, the X-ray tube operated at 15 kV and 350 W, and pass energy of 23.5 eV). The C 1s photoelectron line (binding energy = 284.6 eV) was used to calibrate the photoelectron binding energies. A PANalytical Empyrean X-ray diffractometer with Cu-K α radiation ($\lambda = 1.54 \text{ \AA}$) was used for X-ray diffraction (XRD) analysis. The operating voltage of the X-ray tube was 40 kV and the current was 40 mA. To study the surface morphology and chemical composition of the synthesized Rh@GO-NH₂, 3D morphological images of the samples were taken with a Zeiss Sigma 300 model field emission scanning electron microscope (FE-SEM) equipped with energy dispersive X-ray spectroscopy (EDS) and an In-Lens (SE1) detector operating at a 10 kV acceleration voltage.

2.2 Preparation of Amine-Functionalized Graphene Oxide (GO-NH₂)

Initially, graphene oxide (GO) was synthesized by the Hummer's method via the oxidation of graphite powder with

KMnO₄ and NaNO₃ [47]. Briefly, 5 g of graphite, 115 mL of concentrated H₂SO₄, and 2.5 g of NaNO₃ were combined in an ice bath for 30 min, keeping the temperature below 20 °C. Over a period of 30 min, 15 g of KMnO₄ was gradually added to the mixture and stirred for another hour. After that, the mixture was stirred for an additional hour at 45 °C. 230 mL of distilled water was then added with vigorous stirring for 15 min, followed by continued stirring for 30 min at 45 °C. 600 mL of distilled water and 150 mL of 9% H₂O₂ were added to the resulting mixture and stirred for another hour. The resulting solid product was filtered, washed several times with a 5% HCl solution, and then dried. To synthesize GO-NH₂, 1 g of GO was dispersed in 100 mL of toluene through sonication for 30 min. Then, 2.6 mL of APTES was added to the mixture and stirred at 25 °C for 3 h. The resulting black solid was filtered, washed successively with toluene and ethanol, and then dried [48]. The covalent attachment of APTES occurred through its reaction with the hydroxyl groups present on the basal planes and edges of GO.

2.3 Preparation of Rh@GO-NH₂ Catalyst

The wet-impregnation technique was used to prepare the Rh@GO-NH₂ catalyst. The prepared GO-NH₂ was added to a solution of RhCl₃·H₂O (4.15 mg; 19.8 μmol Rh) in 5.0 mL of water and stirred at 700 rpm for 3 h. The reduction of Rh(III) ions to the Rh(0) NPs was carried out by adding an excess amount of NaBH₄ aqueous solution dropwise until the gas evolution. To remove possible impurities such as metaborate, the resulting Rh@GO-NH₂ product was filtered and washed three times with distilled water, and then dried under vacuum at 100 °C.

2.4 Catalytic Efficiency of Rh@GO-NH₂ in the Nitroarene Reduction

1 mg of Rh@GO-NH₂ was added to a solution of 4-nitrophenol (4-NP) (5 mg) and excess NaBH₄ (30 mg) and stirred at 55 °C. The mixture was stirred until the yellow color of the 4-nitrophenolate solution became colorless, indicating the conversion of 4-NP to 4-aminophenol (4-AP). The progress of the reaction was monitored using a UV–Vis spectrophotometer.

2.5 Reusability Study of the Rh@GO-NH₂ Catalyst

The reusability of the Rh@GO-NH₂ catalyst was studied in two methods; (A) After reduction of 4-NP (5 mg) with NaBH₄ (30 mg) in the presence of 1 mg of catalyst at 55 °C, the Rh@GO-NH₂ catalyst was separated by centrifugation and washed successively with ethanol and water, and dried in a vacuum at 60 °C. A fresh solution of 4-NP and NaBH₄ was added to the recovered catalyst and the reaction was carried out under the same conditions. (B) 1 mg of Rh@GO-NH₂ catalyst was added to a solution of 4-NP (5 mg) and NaBH₄ (30 mg) in 2.5 mL of water and stirred at 55 °C for an appropriate time. After the completion of the reaction, which was monitored by UV–Vis, 2.5 mL of an aqueous solution of 4-NP (5 mg) and NaBH₄ (30 mg) was added to the above mixture without separating the catalyst and then heated at the same temperature. Addition of a fresh solution of 4-NP and NaBH₄ was continued nine times.

3 Results and Discussion

3.1 Characterization of Catalyst

ICP-OES, FE-SEM, SEM-elemental mapping, XRD, XPS, and high-resolution XPS were used to characterize the Rh@GO-NH₂ catalyst. The Rh content of Rh@GO-NH₂ was determined by an ICP-OES analysis, which showed that the Rh content of the catalyst was 1.70 ± 0.01% wt%. SEM was first used to study the morphological analysis of the Rh@GO-NH₂ catalyst. The SEM images and the corresponding EDS spectrum of the Rh@GO-NH₂ catalyst are shown in Fig. 2a–d. There are distinct layers of graphene shown in Fig. 2a–c. The Rh(0) NPs are homogeneously distributed between the graphene layers and on their surface, as shown in Fig. 2c. C, O, N, Si and Rh peaks were shown in the EDS spectrum of the Rh@GO-NH₂ catalyst, revealing the modification of GO by APTES and the immobilization of Rh(0) NPs on the GO surface. The homogenous spots of C, O, N, Si and Rh in the SEM-elemental mapping images of the Rh@GO-NH₂ catalyst confirmed the presence of Rh(0) NPs (Fig. 3c–f).

Powder XRD analysis was performed to assess the crystal structure of the catalyst. The XRD patterns of GO-NH₂ and Rh@GO-NH₂ catalyst are shown in Fig. 4. As can be seen from the figure, the XRD patterns of both the solid support and the catalyst mostly overlap, except for a small shoulder around 40.7° of the Rh@GO-NH₂ sample. It can be understood from the literature that the reflections observed at 2θ = 11.7°, 21.7° and 42.7° in both examples originate from the C (001), C (002) and C (102) planes, respectively [38]. Due to the amorphous structure of graphene, the XRD pattern of the Rh@GO-NH₂ catalyst is broadened [49]. The small deposition of Rh(0) NPs on the GO-NH₂ surface may be responsible for the absence of Rh(0) NPs diffraction peaks.

XPS analysis was performed to ascertain the oxidation state of metallic Rh metal and to determine the surface composition of the Rh@GO-NH₂ catalyst. The XPS study revealed the presence of elements C, O, N, Si, and Rh in the structure of the Rh@GO-NH₂ catalyst (Fig. 5a) The core level XPS spectrum of Rh 3d was deconvoluted into two main peaks observed at approximately 307 eV and 312 eV for Rh 3d_{5/2} and Rh 3d_{3/2}, respectively. The Rh 3d spectra in Fig. 5 (b) indicated mixed metallic (Rh(0)) and oxidized Rh₂O₃ (Rh(III)) phases for the catalyst. The Rh 3d transitions in Fig. 5b showed 3d_{5/2} at 306.9 and 308.8 eV for Rh(0) and Rh(III), respectively; similarly, 3d_{3/2} was at 311.7 and 313.5 eV for Rh(0) and Rh(III), respectively [50–54].

3.2 The Catalytic Efficiency of Rh@GO-NH₂ Catalyst in the Nitroarene Reduction

The catalytic activity of Rh@GO-NH₂ towards the reduction of 4-NP to 4-AP was investigated by treating an aqueous solution of 4-NP (5 mg/5 mL) with 50 mg of NaBH₄ in the presence of the Rh@GO-NH₂ catalyst. A UV–Vis spectrophotometer was used to measure the conversion of 4-NP to 4-AP. However, the conversion of 4-NP to 4-AP could be observed with the naked eye when the solution turned from yellow to colorless during the reaction. The reduction of 4-NP catalyzed by Rh@GO-NH₂ was investigated under different conditions to determine the optimal reaction conditions for the reducing of nitroaromatic compounds. As shown in Table 1 (entries 1–4), increasing the catalyst loading decreased the time required for complete conversion. We decided that 1 mg of catalyst was the optimal amount because it gave almost identical results to the higher amount of catalyst (entry 2). No conversion was observed after 120 min when 0 mg of catalyst was used (entry 1). The time to complete the conversion increased as the amount of NaBH₄ was reduced (entries 5–7). Similar results were obtained using 30 and 50 mg of NaBH₄ (entries 2 and 5). When NaBH₄ was not used, the conversion of 4-NP was less than 5% (entry 7). After 3 h, only 45% reduction of 4-NP

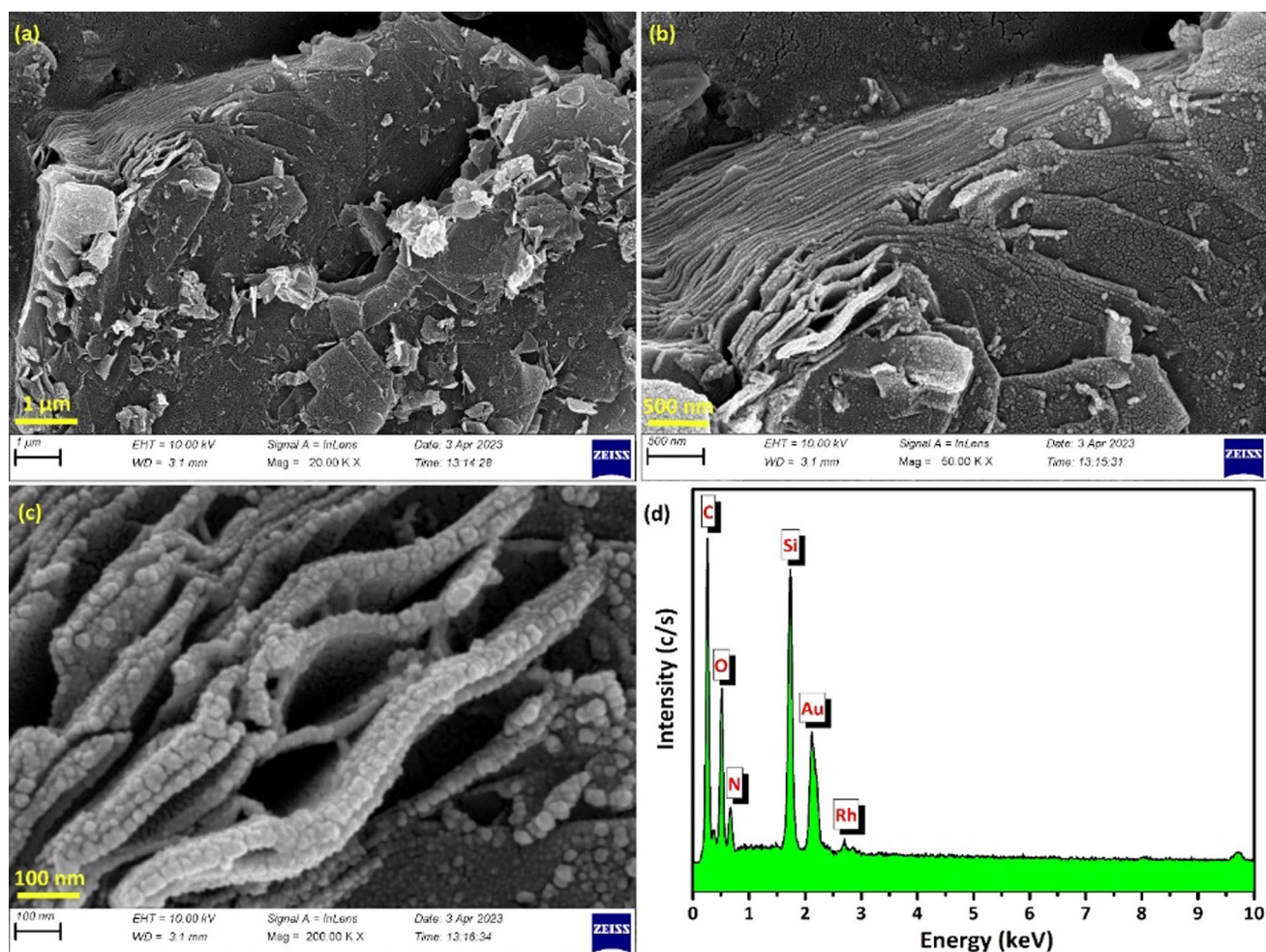


Fig. 2 SEM images in different scale (a–c) and corresponding EDS spectrum (d) of Rh@GO-NH₂ catalyst

reduction was observed when the reaction was performed at room temperature (entry 8). Therefore, the optimal amounts of catalyst, NaBH₄, and temperature were determined to be 1 mg, 30 mg, and 55 °C, respectively (entry 5).

Under optimal reaction conditions, the ability of the Rh@GO-NH₂ catalyst to reduce nitroaromatic compounds containing different functional groups was investigated. Various electron-donating and electron-withdrawing substituted nitroaromatics were treated with Rh@GO-NH₂ and NaBH₄ reductant. The UV–Vis spectra of nitroaromatics before and after the reduction are shown in Fig. 6. Table 2 shows the results of the Rh@GO-NH₂-catalyzed reduction of nitroarene derivatives in terms of time, conversion, and selectivity. Within 30 min, nitrobenzene and 4-nitrotoluene were reduced to the corresponding aniline derivatives with high conversion and 100% selectivity. Rapid reduction of electron-donating substituted nitrobenzene derivatives, including 4-nitrophenol (4-NP), 2-nitroaniline, 4-nitroaniline, and 4-chloro-2-nitroaniline, resulted in > 99% conversion with 100% selectivity to the

corresponding aniline derivatives. In the case of nitrobenzaldehyde, nitroacetophenone and nitrobenzoic acid derivatives, electron-withdrawing groups such as formyl, acetyl, and carboxyl caused their reduction to the corresponding anilines in longer time (30–90 min). The main products were the corresponding aminobenzyl alcohols of nitrobenzaldehyde and nitroacetophenone derivatives. However, the selectivity of 2-nitro and 3-nitrobenzaldehydes to the corresponding aminobenzaldehydes was low.

The synthetic utility of this method was demonstrated by reduction of nitrobenzene with NaBH₄ in the presence of Rh@GO-NH₂, followed by in situ treatment with formic acid or acetic acid. Treatment of nitrobenzene with excess NaBH₄ in the presence of Rh@GO-NH₂ catalyst at 55 °C led to the in-situ formation of aniline, which was then transformed to the corresponding formanilide and acetanilide in 76% and 83% isolated yields, when reacted with formic acid and acetic acid and heated at 90 °C for 5 h, respectively. Cascade Rh@GO-NH₂-catalyzed reduction of 2-nitroaniline and treatment with formic acid under

Fig. 3 SEM image (a), and elemental mapping C (b), O (c), N (d), Si (e) and Rh (f) of Rh@GO-NH₂ catalyst

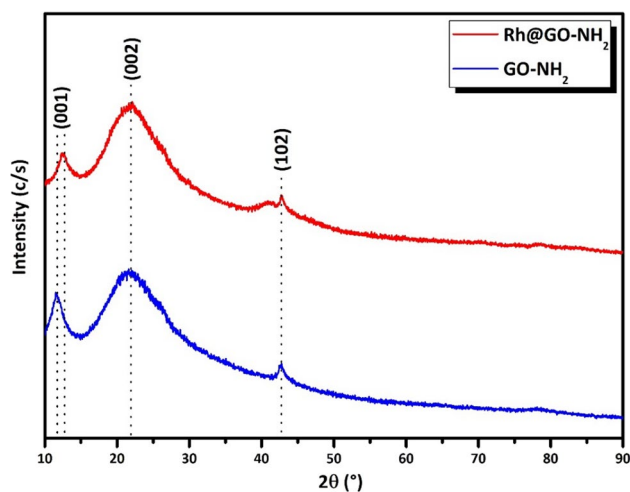
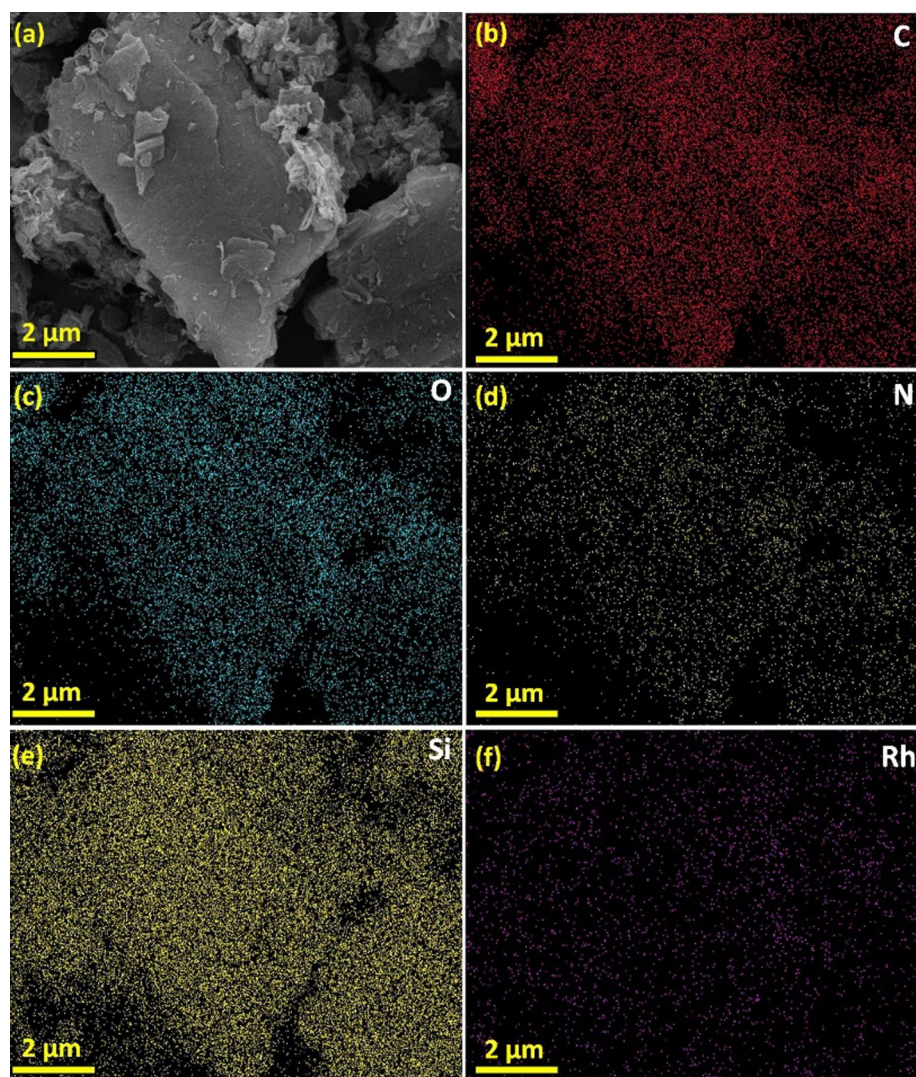


Fig. 4 XRD pattern of GO-NH₂ and Rh@GO-NH₂ samples

similar reaction conditions afforded benzimidazole in 66% yield (Scheme 1).

The recyclability of the Rh@GO-NH₂ catalyst was investigated in two ways. In the first method (A), after the completing the reduction of 4-NP (5 mg) with NaBH₄ (30 mg) in the presence of catalyst (1 mg) at 55 °C, the catalyst was separated by centrifugation and washed twice with water and ethanol. The isolated catalyst was treated with a fresh solution of 4-NP and NaBH₄ in water under the same reaction conditions. The catalyst was reused 4 times without significant loss of activity. In another method (B), 1 mg of Rh@GO-NH₂ catalyst was treated with a solution of 4-NP (5 mg) and NaBH₄ (30 mg) in water (2.5 mL) at 55 °C, and then when the reaction was completed, a new solution of reagents (5 mg of 4-NP and 30 mg of NaBH₄ in 2.5 mL of water) was added to the mixture without separating the catalyst and the reaction continued under the same conditions. Adding a new solution of reagents was done nine times without separating the catalyst, and the results showed that the Rh@GO-NH₂

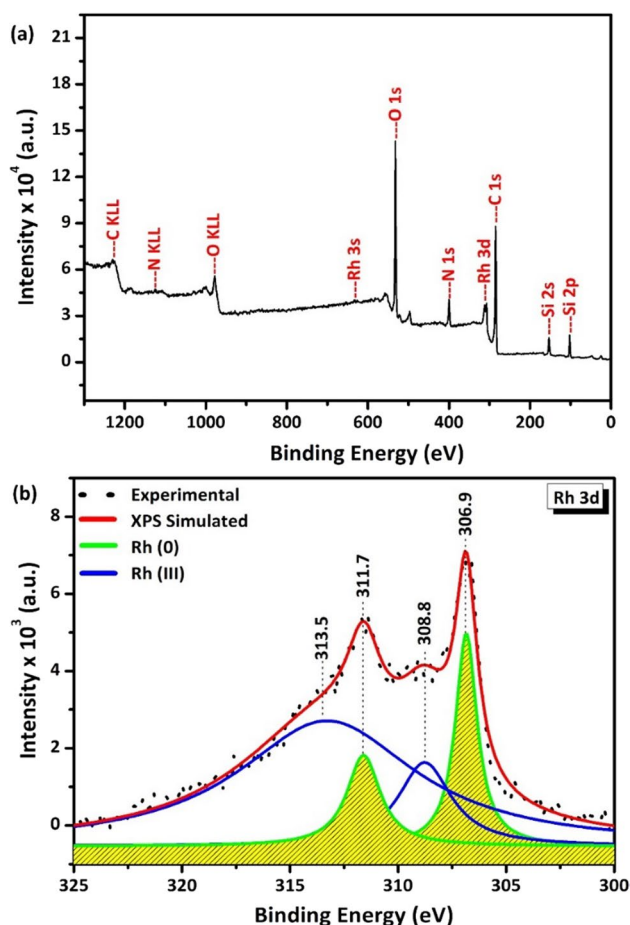


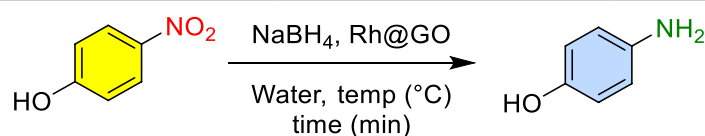
Fig. 5 Survey scan (a) and Rh 3d core level (b) XPS spectra of Rh@GO-NH₂ catalyst

catalyst maintained its catalytic activity for nine times without losing its efficiency. Method A was not repeated more than 4 times due to catalyst loss during separation (Fig. 7b, c). To investigate the structural changes of the catalyst during the reduction of 4-NP, FT-IR spectra of Rh@GO-NH₂ were collected before and after recovery and reused for four runs (Fig. 7e). In the FT-IR spectra of Rh@GO-NH₂, the peak at 1550 cm⁻¹ is due to N-H bending vibrations, and the peaks at 1056 and 702 cm⁻¹ are related to asymmetric and symmetric stretching vibrations of Si-O-Si, respectively. These peaks confirmed the successful modification of GO with APTES to obtain amine-functionalized GO. The band of C-O bonds appeared at 1198 cm⁻¹. As shown in Fig. 7e, the functional groups and structure of the Rh@GO-NH₂ catalyst were preserved after four reusing cycles.

The leaching of Rh species into the reaction mixture was investigated by removing the catalyst after 5 min from the reaction medium of 4-NP and NaBH₄ in water. The reduction was then continued in the absence of catalyst under heating conditions at 55 °C. As shown in Fig. 7d, there was no significant decrease in the absorbance of the mixture at the maximum wavelength of 4-nitrophenolate species at 400 nm, even after 30 min, indicating the heterogeneity of the Rh@GO-NH₂ catalyst.

Table 3 compares the reduction efficiency of 4-nitrophenol or nitrobenzene over the Rh@GO catalyst with some reported works. Table 3 shows that in most cases the reduction of nitroarenes was carried out in alcohol-based solvents and lasted between 1 and 16 h. In addition, in some cases a high temperature was required to reduce nitroarenes. Also, in most cases expensive Rh precursors in combination with other metal precursors at higher

Table 1 Optimization of the conditions for 4-NP reduction^a



Entry	Rh@GO-NH ₂ (mg)	NaBH ₄ (mg)	Temperature (°C)	Time (min)
1	0	50	55	120 ^b
2	1	50	55	15
3	2	50	55	12
4	5	50	55	13
5	1	30	55	15
6	1	15	55	120 ^c
7	1	0	55	120 ^d
8	1	30	rt	180 ^e

^aRh@GO-NH₂ catalyst and NaBH₄ were added to a solution containing 5 mg of 4-NP in 5 mL of water and stirred at temperatures. The reduction of 4-NP was monitored by measuring the absorbance of the solution at the wavelength of maximum absorbance of the 4-nitrophenolate ion using a UV-Vis spectrometer. ^bAfter 120 min, 4-NP remained unchanged in its 4-nitrophenolate form. ^cAbout 65% conversion was observed. ^dLess than 5% conversion was shown. ^eAbout 45% conversion was achieved

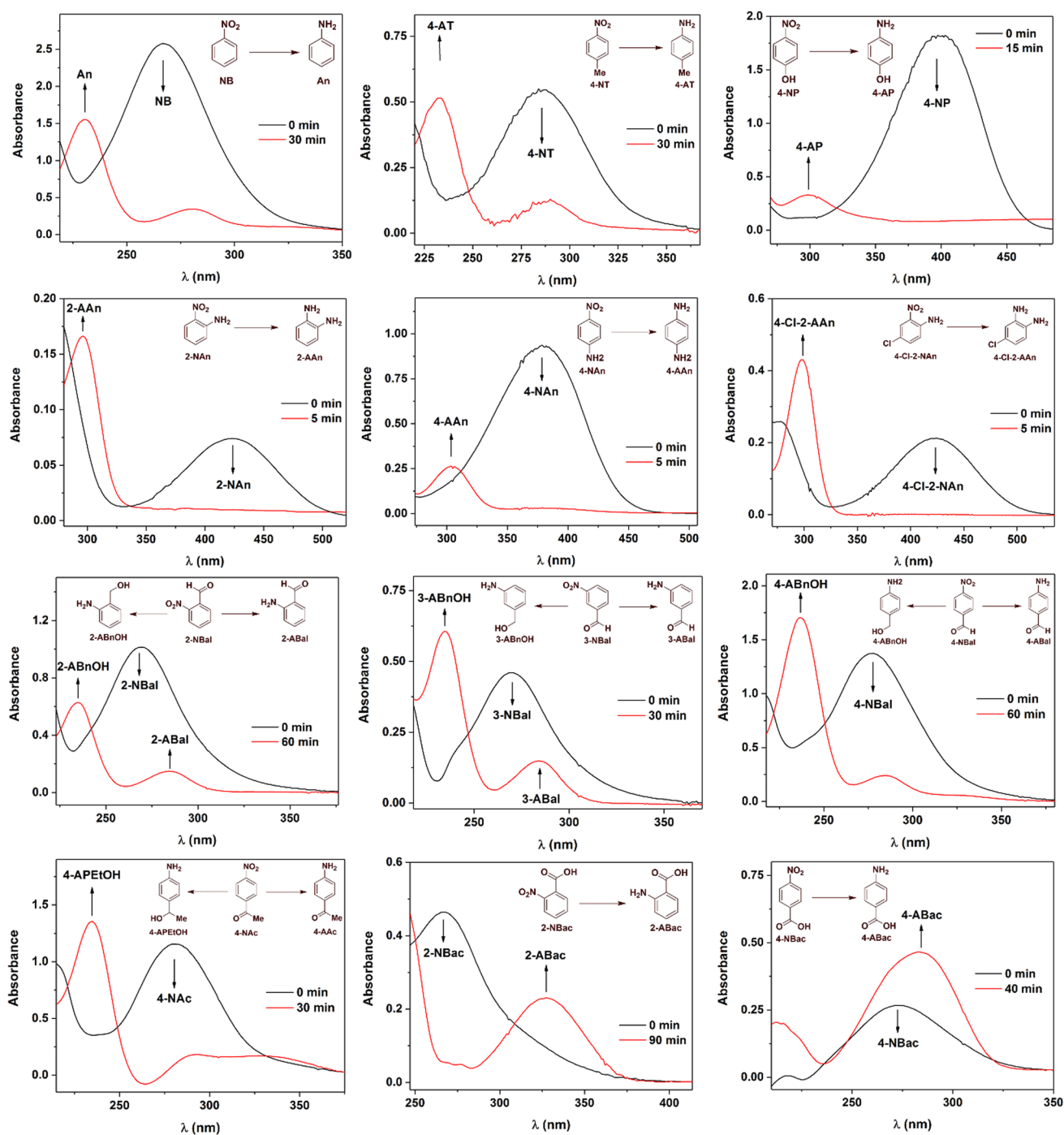


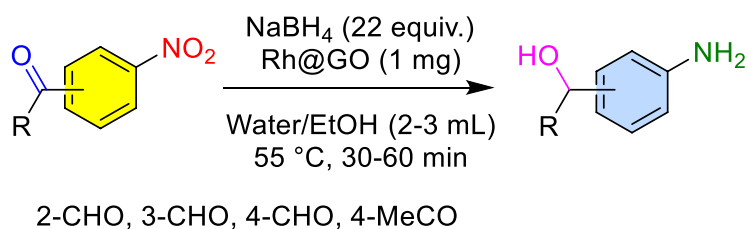
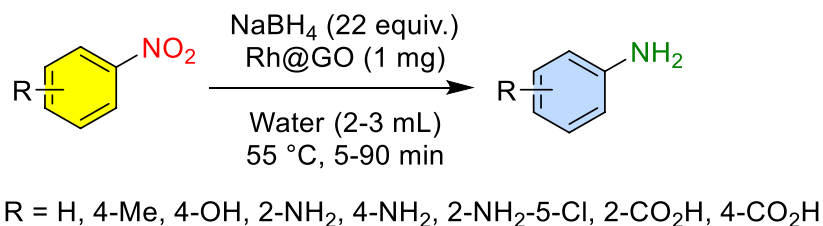
Fig. 6 Rh@GO-NH₂-catalyzed reduction of nitroaromatic compounds, studied with a UV-Vis spectrophotometer at the beginning (0 min) and at the end of the reduction of 4-nitrobenzene, 4-nitrotolu-

ene, 4-nitrophenol, 2-nitroaniline, 4-nitroaniline, 4-chloro-2-nitroaniline, 2-nitrobenzaldehyde, 3-nitrobenzaldehyde, 4-nitrobenzaldehyde, 4-nitroacetophenone, 2-nitrobenzoic acid and 4-nitrobenzoic acid

temperatures were used to prepare supported Rh NPs. Some of the advantages of the Rh@GO catalyst include excellent conversion and selectivity, ease of preparation, rapid reduction of nitro compounds, heterogeneity, and recoverability of the catalyst.

4 Conclusions

In summary, amine-functionalized graphene oxide-decorated Rh(0) NPs were prepared and their catalytic

Table 2 Scope of the Rh@GO-catalyzed reduction of nitroarene derivatives^a

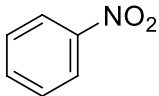
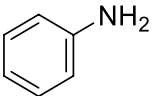
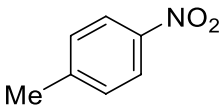
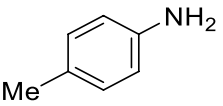
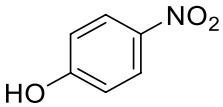
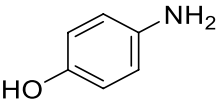
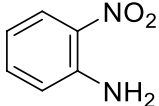
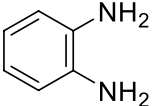
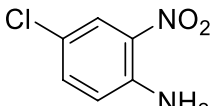
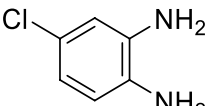
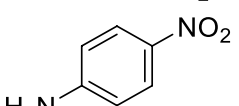
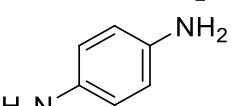
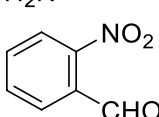
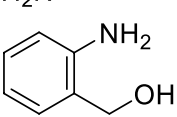
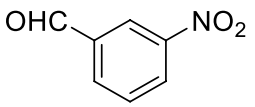
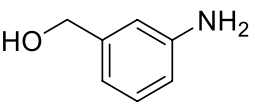
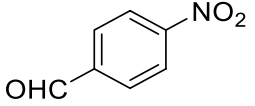
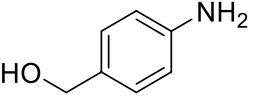
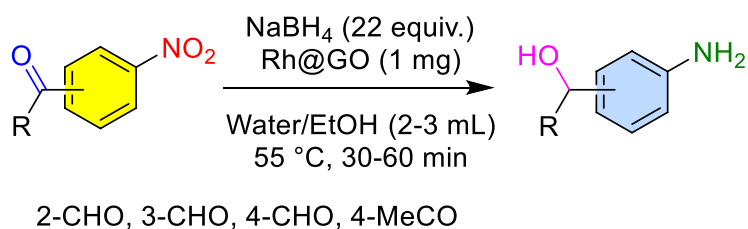
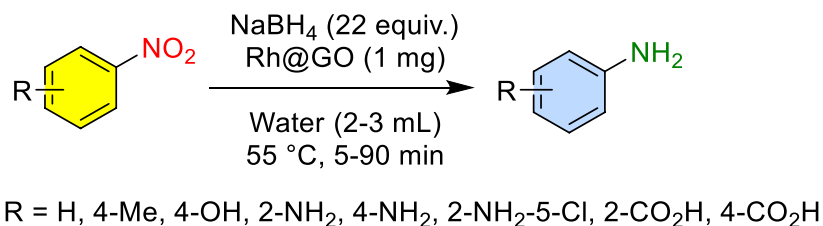
Entry	Nitroarene	Product	Time (min)	Conversion ^c %	Selectivity ^c %
1			30	96	100
2			30	92	100
3			15	>99	100
4			5	>99	100
5			5	>99	100
6			5	>99	100
7			60 ^b	>99	84
8			30 ^b	>99	91
9			60 ^b	92	100

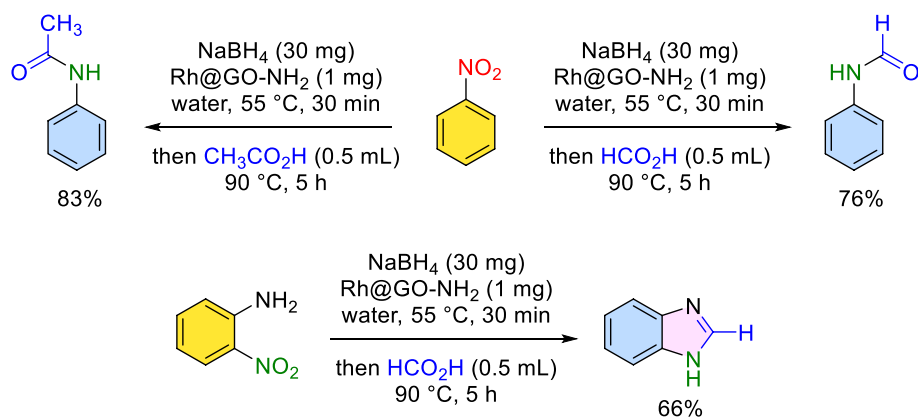
Table 2 (continued)



Entry	Nitroarene	Product	Time (min)	Conversion ^c %	Selectivity ^c %
10			30 ^b	>99	100
11			90 ^b	93	100
12			40 ^b	87	100

^aReaction conditions: Nitroarene (0.035 mmol), NaBH₄ (0.8 mmol, 30 mg), Rh@GO (1 mg), water (2–3), 55 °C. ^bWater/EtOH (3/1: v/v) mixture was used as solvent. ^cConversion and selectivity were determined using GC analysis

Scheme 1 Synthetic utility of Rh@GO catalyzed tandem reduction of nitroarenes and their reaction with formic and acetic acid



activity for the reduction of nitroarene derivatives was investigated. SEM images showed that the Rh(0) NPs were uniformly distributed on and inside the GO sheets.

In addition, the presence of Rh NPs on the surface of the GO layers was confirmed by EDS and elemental mapping analysis. The presence of Rh(0) NPs was further confirmed

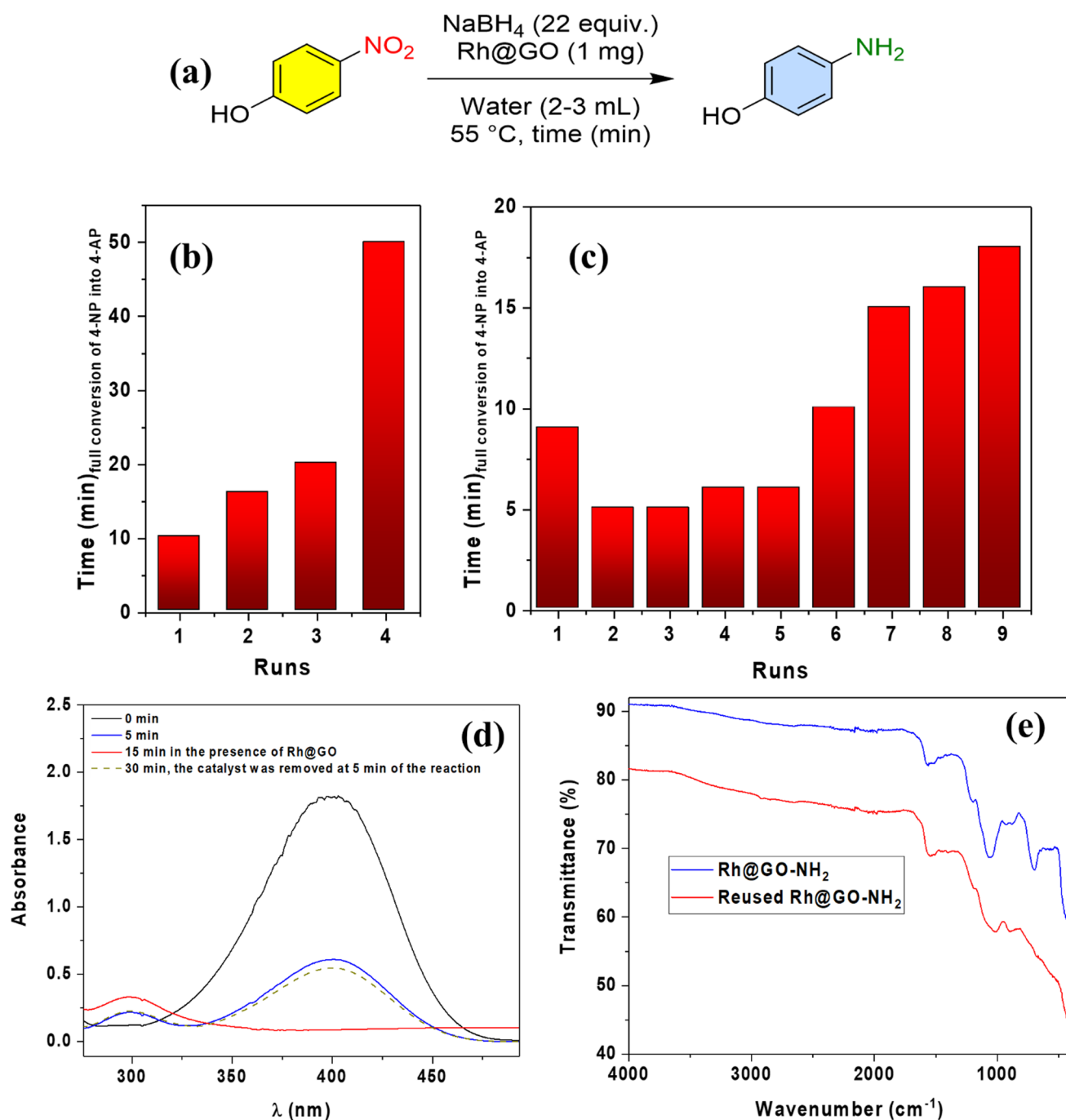


Fig. 7 Reusability of Rh@GO-NH₂ catalyst in the reduction of 4-NP through separating of catalyst (method A) (b) and without catalyst separation (method B) (c), the leaching test of the Rh@GO catalyst

in the reduction of 4-NP (d), and Ft-IR spectra of the Rh@GO-NH₂ catalyst and reused catalyst (e), (Reaction conditions are illustrated in the Scheme a)

by XPS analysis, which showed peaks at binding energies of 306.9 and 311.7 eV. Rh@GO-NH₂ exhibited excellent catalytic activity for the reduction of nitroaromatic compounds using NaBH₄ in aqueous solutions. Strong electron-donating substituted nitroaromatics underwent rapid reduction (5–15 min), while methyl and electron-withdrawing substituted nitroarenes were reduced in

30–90 min. In the case of aldehyde and ketone functional groups, the reduction of carbonyl groups to the corresponding alcohols occurred in addition to the nitro group. The synthetic utility of the Rh@GO-catalyzed tandem reduction of nitroarenes and reaction with formic acid and acetic acid was also studied, leading to the delivery of the corresponding anilide and benzimidazole derivatives. The

Table 3 Comparison of 4-nitrophenol reduction efficiency of Rh@GO with some reported Rh, Au and Pd NPs catalysts

Catalyst (amount, wt% of metal)	Conditions	Conversion, selectivity	References
Fe ₃ O ₄ @SiO ₂ -NH ₂ -RhNPs@mSiO ₂ (40 mg, 0.23mmol% Rh)	H ₂ (1 atm.), <i>i</i> -PrOH, rt, 16 h	> 99%, 100%	[55]
0.5wt%Rh-PAA/Al ₂ O ₃ -TMPM (100 mg)	H ₂ (20 bar), abs. EtOH, rt, 2 h	94.7%, 100% ^a	[56]
Au/TiO ₂ -VS (1 mol% Au)	CO (5 atm), EtOH/H ₂ O, 25 °C, 1 h	99%, 99%	[57]
Fe ₂ O ₃ @HAP-Pd (40 mg)	HCO ₂ NH ₄ , EtOH, 60 °C, 3 h	100%, > 99% ^a	[58]
Pd/Fe ₃ O ₄ @C (40 mg)	NaBH ₄ , MeOH, 60 °C, 1 h	100%, 99% ^a	[59]
Polymeric PEG35k-Pd NPs (1 mol% Pd)	N ₂ H ₄ ·H ₂ O, 90° C, 1–2 h	98% ^b	[60]
Pd-gCN (5 mol% Pd)	N ₂ H ₄ ·H ₂ O, EtOH, 70 °C, 4 h	96% ^b	[61]
PtRh alloy (0.02 mg PtRh)	NaBH ₄ , H ₂ O, rt, ~ 20 min	100%	[43]
RhAg@rGO (0.2 mol% RhAg)	NaBH ₄ , H ₂ O, 20 °C, ~ 15 min	100%	[45]
Rh@GO (1 mg, 1.7 wt% Rh)	NaBH ₄ , H ₂ O, 55 °C, 15 min	100%, > 99%	This work

^aNitrobenzene conversion and selectivity to aniline. ^bIsolated yields

recovered catalyst demonstrated reusability for nine runs without significant loss of catalytic activity. A leaching test was conducted, revealing the heterogeneous properties of the Rh@GO-NH₂ catalyst.

Acknowledgements This study was supported by University of Maragheh and Van Yuzuncu Yil University.

Author Contributions N.P. and A.R. performed the experiments. B.E.S. and M.G. conceived the concept, designed and organized the experiments, supervised the work and wrote the manuscript.

Funding The authors declare that no funds or grants were received during the preparation of this manuscript.

Data Availability The datasets generated during and/or analysed during the current study are available from the corresponding author on reasonable request.

Declarations

Competing Interests The authors have no relevant financial or non-financial interests to disclose.

References

1. F.T. Alshorifi, S.L. Ali, R.S. Salama, Promotional synergistic effect of Cs–Au NPs on the performance of Cs–Au/MgFe₂O₄ catalysts in catalysis 3, 4-Dihydropyrimidin-2 (1H)-Ones and degradation of RhB Dye. *J. Inorg. Organomet. Polym. Mater.* **32**, 3765–3776 (2022)
2. Y. Zhao, L. Lin, M. Hong, Nitrobenzene contamination of groundwater in a petrochemical industry site. *Front. Environ. Sci. Eng.* **13**, 1–9 (2019)
3. S. Ahmadi, Y. Fatahi, M.R. Saeb, D. Kim, M. Shokouhimehr, S. Iravani, N. Rabiee, R.S. Varma, Metal-organic frameworks (MOFs) and their applications in detection, conversion, and depletion of nitroaromatic pollutants. *Inorg. Chem. Commun.* **160**, 111982 (2023)
4. Y.-J. Chen, X.-J. Zhai, W.-L. Wu, B. Li, L.-Y. Wang, Cd (II)-based complex constructed from 1, 3, 5-Tris (Carboxymethoxy)

- benzene acid ligand for detection of nitroaromatic compounds. *J. Inorg. Organomet. Polym. Mater.* **33**, 1409–1414 (2023)
5. X. Li, J. Xie, C. Jiang, J. Yu, P. Zhang, Review on design and evaluation of environmental photocatalysts. *Front. Environ. Sci. Eng.* **12**, 1–32 (2018)
6. J. Meng, M. Ren, S. Wang, J. Gao, X. Shan, J. Hu, A smart adsorbent with ability of environmentally friendly regeneration for p-nitrophenol removal in aqueous solution. *J. Inorg. Organomet. Polym. Mater.* **31**, 2381–2392 (2021)
7. M. Dogan, F. Temel, M. Tabakci, High-performance adsorption of 4-nitrophenol onto calix [6] arene-tethered silica from aqueous solutions. *J. Inorg. Organomet. Polym. Mater.* **30**, 4191–4202 (2020)
8. K. Anand, V. Murugan, S. Mohana Roopan, T.V. Surendra, A.A. Chuturgoon, S. Muniyasamy, Degradation treatment of 4-nitrophenol by Moringa oleifera synthesised GO-CeO₂ nanoparticles as catalyst. *J. Inorg. Organomet. Polym. Mater.* **28**, 2241–2248 (2018)
9. H. Zeng, L. Lu, M. Liang, J. Liu, Y. Li, Degradation of trace nitrobenzene in water by microwave-enhanced H₂O₂-based process. *Front. Environ. Sci. Eng.* **6**, 477–483 (2012)
10. K.-S. Ju, R.E. Parales, Nitroaromatic compounds, from synthesis to biodegradation. *Microbiol Mol Biol Rev.* **74**, 250–272 (2010)
11. P. Liu, Y. Liu, Y. Lv, W. Xiong, F. Hao, H. Luo, Zinc modification of Ni-Ti as efficient Ni x Zn y Ti1 catalysts with both geometric and electronic improvements for hydrogenation of nitroaromatics. *Front. Chem. Sci. Eng.* **16**, 461–474 (2022)
12. K. Zhang, J.M. Suh, J.-W. Choi, H.W. Jang, M. Shokouhimehr, R.S. Varma, Recent advances in the nanocatalyst-assisted NaBH₄ reduction of nitroaromatics in water. *ACS Omega* **4**, 483–495 (2019)
13. A. Akbari, M. Amini, A. Tarassoli, B. Eftekhari-Sis, N. Ghasemian, E. Jabbari, Transition metal oxide nanoparticles as efficient catalysts in oxidation reactions. *Nano-Struct. Nano-Object* **14**, 19–48 (2018)
14. K. Yavari, B. Eftekhari-Sis, A.J.N. Akbari, Synthesis and application of silver and cobalt nanoparticles immobilized on ionic liquid-functionalized halloysite nanotubes in the reduction of 4-nitrophenol in aqueous solution. *NANO* **16**, 2150089 (2021)
15. A. Akbari, A. Naderahmadian, B.J.P. Eftekhari-Sis, Silver and copper nanoparticles stabilized on ionic liquids-functionalized polyhedral oligomeric silsesquioxane (POSS): highly active and recyclable hybrid catalysts. *Polyhedron* **171**, 228–236 (2019)

16. A.I. Raafat, G.A. Mahmoud, T.B. Mostafa, Efficient catalytic reduction of hazardous anthropogenic pollutant, 4-nitrophenol using radiation synthesized (polyvinyl pyrrolidone/acrylic acid)-silver nanocomposite hydrogels. *J. Inorg. Organomet. Polym. Mater.* **30**, 3116–3125 (2020)
17. B. Paul, D.D. Purkayastha, S.S. Dhar, S. Das, S. Haldar, Facile one-pot strategy to prepare Ag/Fe₂O₃ decorated reduced graphene oxide nanocomposite and its catalytic application in chemoselective reduction of nitroarenes. *J. Alloy. Compd.* **681**, 316–323 (2016)
18. A. George, D. Selvan, S. Mandal, Catalytic reduction of toxic nitroarenes in aqueous medium using worm-like rhodium nanoparticles. *ChemistrySelect* **2**, 9718–9721 (2017)
19. M.A. Bhosale, S.S.R. Gupta, B.M. Bhanage, Size controlled synthesis of gold nanostructures using ketones and their catalytic activity towards reduction of p-nitrophenol. *Polyhedron* **120**, 96–102 (2016)
20. G. Kibar, A. Tuncel, Gold-nanoparticle decorated monosized magnetic polymer based catalyst: reduction of 4-nitrophenol. *J. Inorg. Organomet. Polym. Mater.* **28**, 2249–2257 (2018)
21. A. Nasri, B. Jaleh, Z. Nezafat, M. Nasrollahzadeh, S. Azizian, H.W. Jang, M. Shokouhimehr, Fabrication of g-C₃N₄/Au nanocomposite using laser ablation and its application as an effective catalyst in the reduction of organic pollutants in water. *Ceram. Int.* **47**, 3565–3572 (2021)
22. U. Mahanitipong, S. Chanthip, M. Rutnakornpituk, Carboxymethyl chitosan-magnetite nanocomposites immobilized with Pd as reusable catalysts for the reduction of 4-nitrophenol and methylene blue. *J. Inorg. Organomet. Polym. Mater.* **33**, 1716–1728 (2023)
23. A. Kim, S.M. Rafiaei, S. Abolhosseini, M. Shokouhimehr, Palladium nanocatalysts confined in mesoporous silica for heterogeneous reduction of nitroaromatics. *Energy Environ. Focus* **4**, 18–23 (2015)
24. M. Sajjadi, N.Y. Baran, T. Baran, M. Nasrollahzadeh, M.R. Tahsili, M. Shokouhimehr, Palladium nanoparticles stabilized on a novel Schiff base modified Unye bentonite: highly stable, reusable and efficient nanocatalyst for treating wastewater contaminants and inactivating pathogenic microbes. *Sep. Purif. Technol.* **237**, 116383 (2020)
25. Z. Ali, O. Ghazy, G. Meligi, H. Saleh, M. Bekhit, Copper nanoparticles: synthesis, characterization and its application as catalyst for p-nitrophenol reduction. *J. Inorg. Organomet. Polym. Mater.* **28**, 1195–1205 (2018)
26. Z. Derikvand, A. Azadbakht, H. Amiri Rudbari, Synthesis, characterization, crystal structure and supramolecular interactions of a new Ni (II) compound based on l-histidine and dipicolinic acid; new solid state precursor for NiO nanoparticles and its catalytic activity for nitrophenol reduction. *J. Inorg. Organomet. Polym. Mater.* **29**, 502–516 (2019)
27. S.R. Khan, M. Batool, S. Jamil, S. Bibi, S. Abid, M.R.S.A. Janjua, Synthesis and characterization of Mg–Zn bimetallic nanoparticles: selective hydrogenation of p-nitrophenol, degradation of reactive carbon black 5 and fuel additive. *J. Inorg. Organomet. Polym. Mater.* **30**, 438–450 (2020)
28. G. Wei, J. Zhang, J. Luo, H. Xue, D. Huang, Z. Cheng, X. Jiang, Nanoscale zero-valent iron supported on biochar for the highly efficient removal of nitrobenzene. *Front. Environ. Sci. Eng.* **13**, 1–11 (2019)
29. S.H. Sharfand, S.J. Hoseini, M. Bahrami, Ionic liquid-assisted synthesis of Pt nano thin films at toluene–water interface: enhanced CO tolerance in methanol fuel cells and adsorptive removal of p-nitrophenol from water. *Polyhedron* **151**, 483–497 (2018)
30. V. Rahimkhoei, A. Akbari, M. Zirak, B. Eftekhari-Sis, Ag nanoparticles stabilized on cubic polyhedral oligomeric silsesquioxane cross-linked poly (N-isopropyl acrylamide-co-itaconic acid): an efficient catalyst for 4-nitrophenol reduction. *Funct. Mater. Lett.* **13**, 2051040 (2020)
31. M.A. Bhosale, D.R. Chenna, B.M. Bhanage, Ultrasound assisted synthesis of gold nanoparticles as an efficient catalyst for reduction of various nitro compounds. *ChemistrySelect* **2**, 1225–1231 (2017)
32. S. Ogasawara, S. Kato, Palladium nanoparticles captured in microporous polymers: a tailor-made catalyst for heterogeneous carbon cross-coupling reactions. *J. Am. Chem. Soc.* **132**, 4608–4613 (2010)
33. M. Dhiman, B. Chalke, V. Polshettiwar, Efficient synthesis of monodisperse metal (Rh, Ru, Pd) nanoparticles supported on fibrous nanosilica (KCC-1) for catalysis. *ACS Sustain. Chem. Eng.* **3**, 3224–3230 (2015)
34. Y. Karataş, A. Zengin, M. Gülcan, Pd-doped flower like magnetic MnFe₂O₄ spinel ferrite nanoparticles: synthesis, structural characterization and catalytic performance in the hydrazine-borane methanolysis. *J. Energy Inst.* **110**, 101360 (2023)
35. J. Zhu, J. Zhou, T. Zhao, X. Zhou, D. Chen, W. Yuan, Carbon nanofiber-supported palladium nanoparticles as potential recyclable catalysts for the Heck reaction. *Appl. Catal. A* **352**, 243–250 (2009)
36. M.J. Allen, V.C. Tung, R.B. Kaner, Honeycomb carbon: a review of graphene. *Chem. Rev.* **110**, 132–145 (2010)
37. S. Navalon, A. Dhakshinamoorthy, M. Alvaro, H. Garcia, Carbocatalysis by graphene-based materials. *Chem. Rev.* **114**, 6179–6212 (2014)
38. H.G. Soğukömeroğulları, Y. Karataş, M. Celebi, M. Gülcan, M. Sönmez, M. Zahmakiran, Palladium nanoparticles decorated on amine functionalized graphene nanosheets as excellent nanocatalyst for the hydrogenation of nitrophenols to aminophenol counterparts. *J. Hazard. Mater.* **369**, 96–107 (2019)
39. H. Daneshafroz, H. Barani, H. Sheibani, Palladium nanoparticles-decorated β-cyclodextrin–cyanoguanidine modified graphene oxide: a heterogeneous nanocatalyst for suzuki–miyaura coupling and reduction of 4-nitrophenol reactions in aqueous media. *J. Inorg. Organomet. Polym. Mater.* **32**, 791–802 (2022)
40. L. Xu, D. Liu, D. Chen, H. Liu, J. Yang, Size and shape controlled synthesis of rhodium nanoparticles. *Heliyon* **5**, e01165 (2019)
41. S.B. Kim, Catalysis application of metal (Rh, Ir) quinonoid complexes. *J. Inorg. Organomet. Polym. Mater.* **24**, 58–65 (2014)
42. P. Luo, K. Xu, R. Zhang, L. Huang, J. Wang, W. Xing, J. Huang, Highly efficient and selective reduction of nitroarenes with hydrazine over supported rhodium nanoparticles. *Catal. Sci. Technol.* **2**, 301–304 (2012)
43. Q. Yan, X.-Y. Wang, J.-J. Feng, L.-P. Mei, A.-J. Wang, Simple fabrication of bimetallic platinum–rhodium alloyed nano-multipods: a highly effective and recyclable catalyst for reduction of 4-nitrophenol and rhodamine B. *J. Colloid Interface Sci.* **582**, 701–710 (2021)
44. Z. Hu, J. Zhou, Y. Ai, L. Liu, L. Qi, R. Jiang, H. Bao, J. Wang, J. Hu, H.-B. Sun, Two dimensional Rh/Fe₃O₄/g-C₃N₄-N enabled hydrazine mediated catalytic transfer hydrogenation of nitroaromatics: a predictable catalyst model with adjoining Rh. *J. Catal.* **368**, 20–30 (2018)
45. C. Wang, R. Ciganda, L. Yate, S. Moya, L. Salmon, J. Ruiz, D. Astruc, RhAg/rGO nanocatalyst: ligand-controlled synthesis and superior catalytic performances for the reduction of 4-nitrophenol. *J. Mater. Sci.* **52**, 9465–9476 (2017)
46. B. Paul, S. Vadivel, N. Yadav, S.S. Dhar, Room temperature catalytic reduction of nitrobenzene to azoxybenzene over one pot synthesised reduced graphene oxide decorated with Ag/ZnO nanocomposite. *Catal. Commun.* **124**, 71–75 (2019)

47. D.C. Marcano, D.V. Kosynkin, J.M. Berlin, A. Sinitskii, Z. Sun, A. Slesarev, L.B. Alemany, W. Lu, J.M. Tour, Improved synthesis of graphene oxide. *ACS Nano* **4**, 4806–4814 (2010)
48. X. Wang, W. Xing, P. Zhang, L. Song, H. Yang, Y. Hu, Covalent functionalization of graphene with organosilane and its use as a reinforcement in epoxy composites. *Compos. Sci. Technol.* **72**, 737–743 (2012)
49. O. Vargas, Á. Caballero, J. Morales, Enhanced electrochemical performance of maghemite/graphene nanosheets composite as electrode in half and full Li-ion cells. *Electrochim. Acta* **130**, 551–558 (2014)
50. M. Gulcan, Y. Karataş, Synthesized polyvidone-stabilized Rh (0) nanoparticles catalyzed the hydrolytic dehydrogenation of methylamine-borane in ambient conditions. *New J. Chem.* **41**, 11839–11845 (2017)
51. I.E. Ertas, M. Gulcan, A. Bulut, M. Yurderi, M. Zahmakiran, Rhodium nanoparticles stabilized by sulfonic acid functionalized metal-organic framework for the selective hydrogenation of phenol to cyclohexanone. *J. Mol. Catal. A: Chem.* **410**, 209–220 (2015)
52. S. Günbatar, A. Aygun, Y. Karataş, M. Gülcan, F. Şen, Carbon-nanotube-based rhodium nanoparticles as highly-active catalyst for hydrolytic dehydrogenation of dimethylamineborane at room temperature. *J. Colloid Interface Sci.* **530**, 321–327 (2018)
53. M. Kanat, Y. Karataş, M. Gülcan, B. Anıl, Preparation and detailed characterization of zirconia nanopowder supported rhodium (0) nanoparticles for hydrogen production from the methanolysis of methylamine-borane in room conditions. *Int. J. Hydrogen Energy* **43**, 22548–22556 (2018)
54. M. Çelebi, A. Rüzgar, Y. Karataş, M. Gülcan, Manganese oxide octahedral molecular sieves stabilized Rh nanoparticles for the hydrogen production from the ethylenediamine-bisborane hydrolysis. *Int. J. Hydrogen Energy* **47**, 16494–16506 (2022)
55. H. Tian, J. Zhou, Y. Li, Y. Wang, L. Liu, Y. Ai, Z.N. Hu, J. Li, R. Guo, Z. Liu, Rh catalyzed selective hydrogenation of nitroarenes under mild conditions: understanding the functional groups attached to the nanoparticles. *ChemCatChem* **11**, 5543–5552 (2019)
56. C.H. Campos, E. Rosenberg, J.L. Fierro, B.F. Urbano, B.L. Rivas, C.C. Torres, P. Reyes, Hydrogenation of nitro-compounds over rhodium catalysts supported on poly [acrylic acid]/Al₂O₃ composites. *Appl. Catalysis A General* **489**, 280–291 (2015)
57. L. He, L.C. Wang, H. Sun, J. Ni, Y. Cao, H.Y. He, K.N. Fan, Efficient and selective room-temperature gold-catalyzed reduction of nitro compounds with CO and H₂O as the hydrogen source. *Angew. Chem.* **121**, 9702–9705 (2009)
58. L. Jiang, Z. Zhang, Efficient transfer hydrogenation of nitro compounds over a magnetic palladium catalyst. *Int. J. Hydrogen Energy* **41**, 22983–22990 (2016)
59. N. Mei, B. Liu, Pd nanoparticles supported on Fe₃O₄@ C: an effective heterogeneous catalyst for the transfer hydrogenation of nitro compounds into amines. *Int. J. Hydrogen Energy* **41**, 17960–17966 (2016)
60. V. Yadav, S. Gupta, R. Kumar, G. Singh, R. Lagarkha, Polymeric peg35k-pd nanoparticles: efficient and recyclable catalyst for reduction of nitro compounds. *Synth. Commun.* **42**, 213–222 (2012)
61. D. Nandi, S. Siwal, M. Choudhary, K. Mallick, Carbon nitride supported palladium nanoparticles: an active system for the reduction of aromatic nitro-compounds. *Appl. Catal. A* **523**, 31–38 (2016)

Publisher's Note Springer Nature remains neutral with regard to jurisdictional claims in published maps and institutional affiliations.

Springer Nature or its licensor (e.g. a society or other partner) holds exclusive rights to this article under a publishing agreement with the author(s) or other rightsholder(s); author self-archiving of the accepted manuscript version of this article is solely governed by the terms of such publishing agreement and applicable law.